Study of postseismic deformation due to the 2015 M 7.2 Sarez (Pamir) earthquake using Sentinel-1 InSAR observations

Zeyu Jin, Yuri Fialko, Institute of Geophysics and Planetary Physics, Scripps Institution of Oceanography, University of California, San Diego

zej011@ucsd.edu   yfialko@ucsd.edu

Coseismic deformation from InSAR obversations

Figure 2: Unwrapped interferograms (left column) and pixel offsets in range and azimuth direction (central and right columns). The blue star indicates the epicenter. The focal mechanism denotes the GCMT (Global Centroid Moment Tensor catalog) solution for a Mw 7.2 strike-slip mainshock. Since Sentinel-1 data have much higher resolution in range than that in azimuth, and also because interferometric phase is affected by decorrelation and unwrapping errors near the fault, we use range offsets to digitize the fault trace. The magenta line denotes the fault trace digitized from ascending track, and the cyan line denotes the fault trace digitized from descending track. The two traces overlap except in the small decorrelated area to the south of kink in the rupture trace. The data were processed using GMTSAR (Sandwell et al., 2011).

Modeled coseismic deformation

Figure 3: We use two linear fault segments (magenta lines) digitized from range offsets to approximate the earthquake rupture with two rectangular dislocations in a homogeneous elastic half space (Okada,1985). The applied slip is constrained by seismic moment from GCMT catalog (7.8 x 10^19 N m). Despite a simplified geometry, the model predictions look similar to the observations (left column in Figure 2). Even though there is some near-field difference between modeled and observed displacements, the long wavelength stress changes predicted by the model are sufficiently accurate in the far field. Therefore, this model is adequate as the initial condition for stress-driven postseismic relaxation simulations.

Reference

1. Metzger, Sabrina, et al. Tectonics 36.11 (2017): 2407-2421.
2. Hooper, Andrew, P. Segall, and Howard Zebker. Journal of Geophysical Research: Solid Earth 112.B7 (2007).
3. Sandwell, David, et al. Eos, Transactions American Geophysical Union 92.28 (2011): 234-234.
4. Tymofyeyeva, Ekaterina, and Yuri Fialko. Journal of Geophysical Research: Solid Earth 120.8 (2015): 5952-5963.
4. Fialko, Yuri. Journal of Geophysical Research: Solid Earth 109.B8 (2004).
5. Okada, Yoshimitsu. Bulletin of the seismological society of America 75.4 (1985): 1135-1154.
7. Wang, Rongjiang, Francisco Lorenzo-Martín, and Frank Roth. Computers & Geosciences 32.4 (2006): 527-541.

Overview / Tectonic settings

The Pamir and the Tibetan plateau are a result of a collision between Eurasia and northward advancing India. The western Pamir deforms internally by conjugate strike-slip faulting under north-south compression, together with normal faulting, causing westward extrusion (Figure 1c).

Recent December 7th, Mw 7.2 Sarez earthquake occurred in the Pamir's interior (Figure 1a). The earthquake ruptured an ~80km long, subvertical, sinistral fault from the surface to ~30km depth with a maximum slip of ~3m in the upper crust.

We used Sentinel-1A InSAR data, including 2.5 years of post-earthquake acquisitions from ascending and descending tracks, to investigate postseismic deformaton due to this event.

During this period, a pair of two Mw > 6 earthquakes occurred 100km to the north-east from the epicenter of Sarez earthquake. Our results indicate shallow afterslip, and possible contribution from poroelastic rebound. We do not observe clear signature of long-wavelength deformation expected from visco-elastic relaxation.
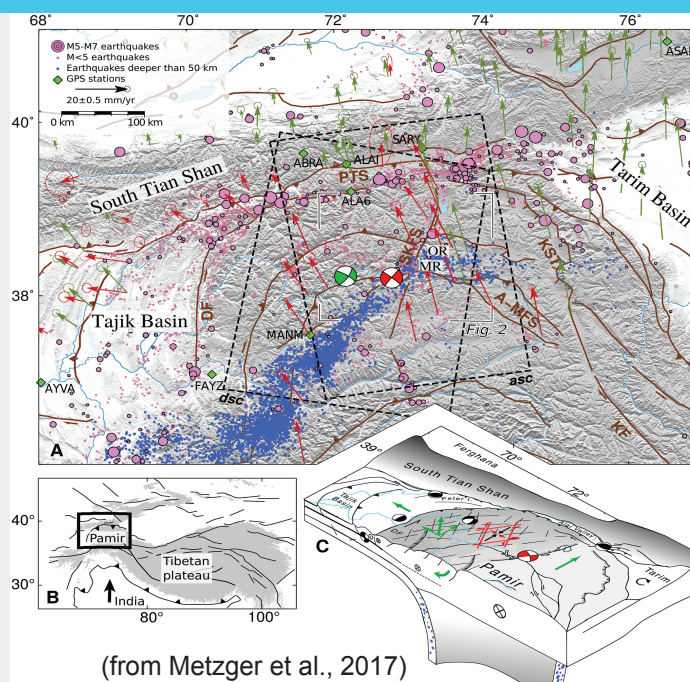

(from Metzger et al., 2017)

Figure 1: tectoincs of Pamir and Tibet

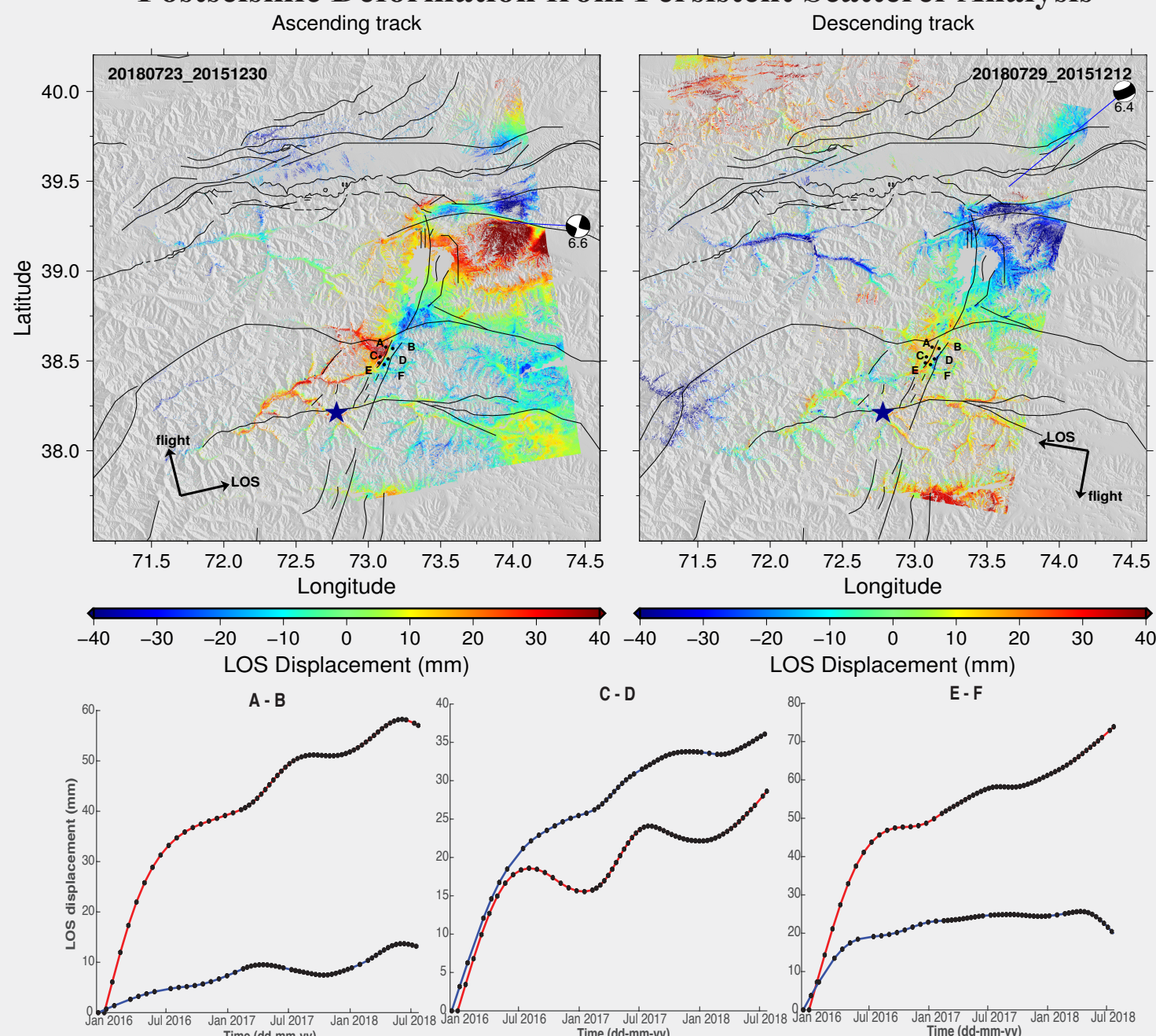## Postseismic Deformation from Persistent Scatterer Analysis

Figure 4: Because the study area is strongly affected by decorrelation due to rugged topography and snow cover, we use Persistent Scatterer method (Hooper et al.,2007) and atmospheric corrections (Tymofyeyeva et al.,2015) to measure time-dependent surface deformation. Top panels show cumulative LOS displacements spanning 2.5 years following the mainshock. The data indicates a sharp step in LOS displacement across the Sarez-Karakul fault (SKF) in ascending track. This discontinuity is not correlated with topography, and therefore likely represents shallow afterslip on the earthquake rupture. There is much smaller signal in descending track because the LOS projection of strike slip is almost zero. We also observe two Mw > 6 aftershocks 100km to the north-east of the mainshock. The shallow afterslip is illustrated in lower panels for three pairs of points across the fault. The red lines represent data from ascending track, while the blue lines represent data from descending track.

Conclusions

1. We analyzed InSAR data over an area of Mw 7.2 Sarez earthquake spanning 2.5 years after the earthquake. The data indicates shallow afterslip along the SKF at the northern end of earthquake rupture. and only observe localized postseismic deformation across the SKFS fault, Also, the data shows coseismic deformation from two M > 6 earthquakes that occurred 100km to the north-east from the mainshock.

2. We compare the observed surface displacements to predictions of postseismic relaxation due to poroelastic rebound and visco-elastic flow in the ductile substrate. The data allows for some amount of poroelastic rebound, but precludes visco-elastic response assuming viscosity 10^18 Pa s or smaller.

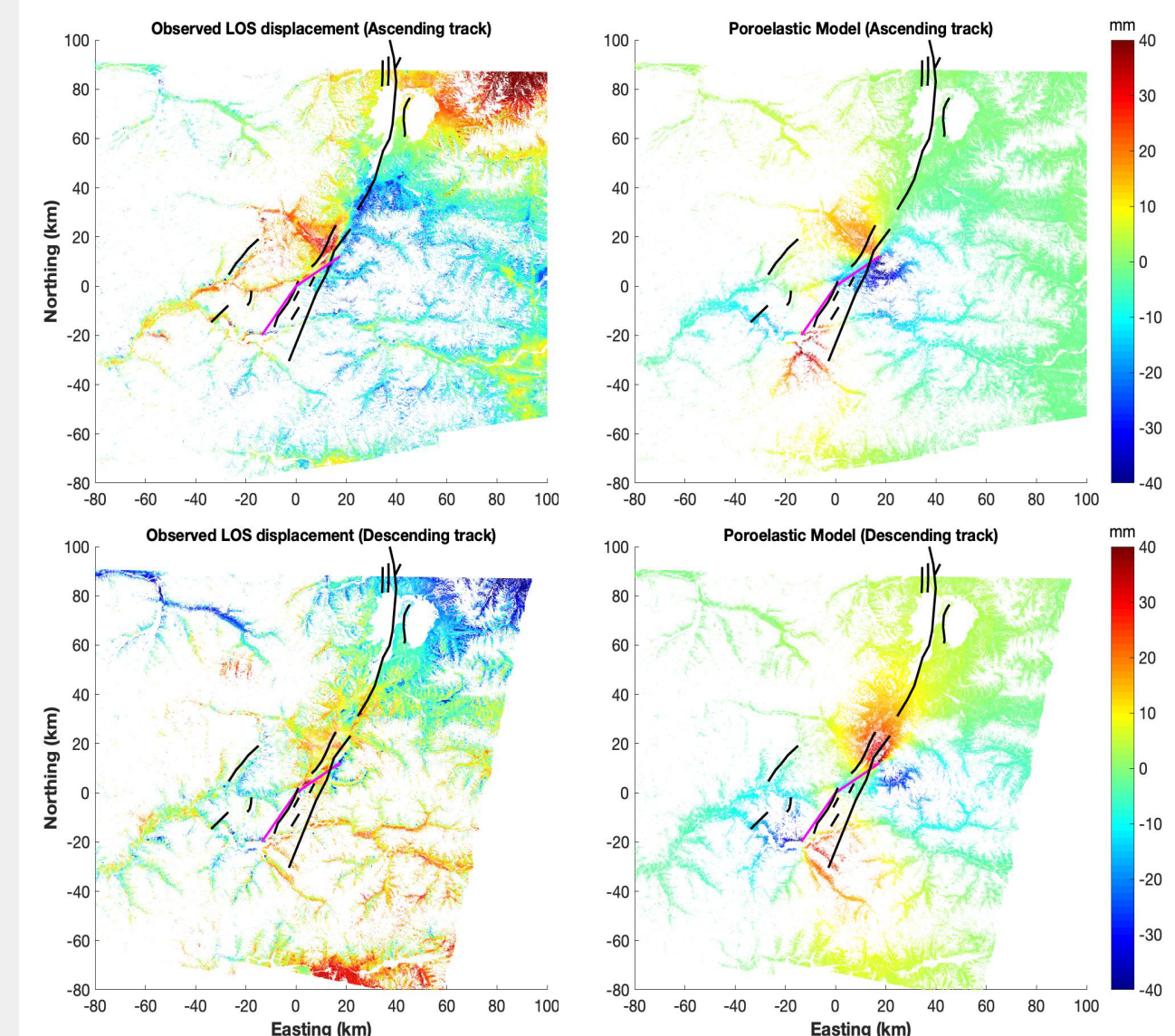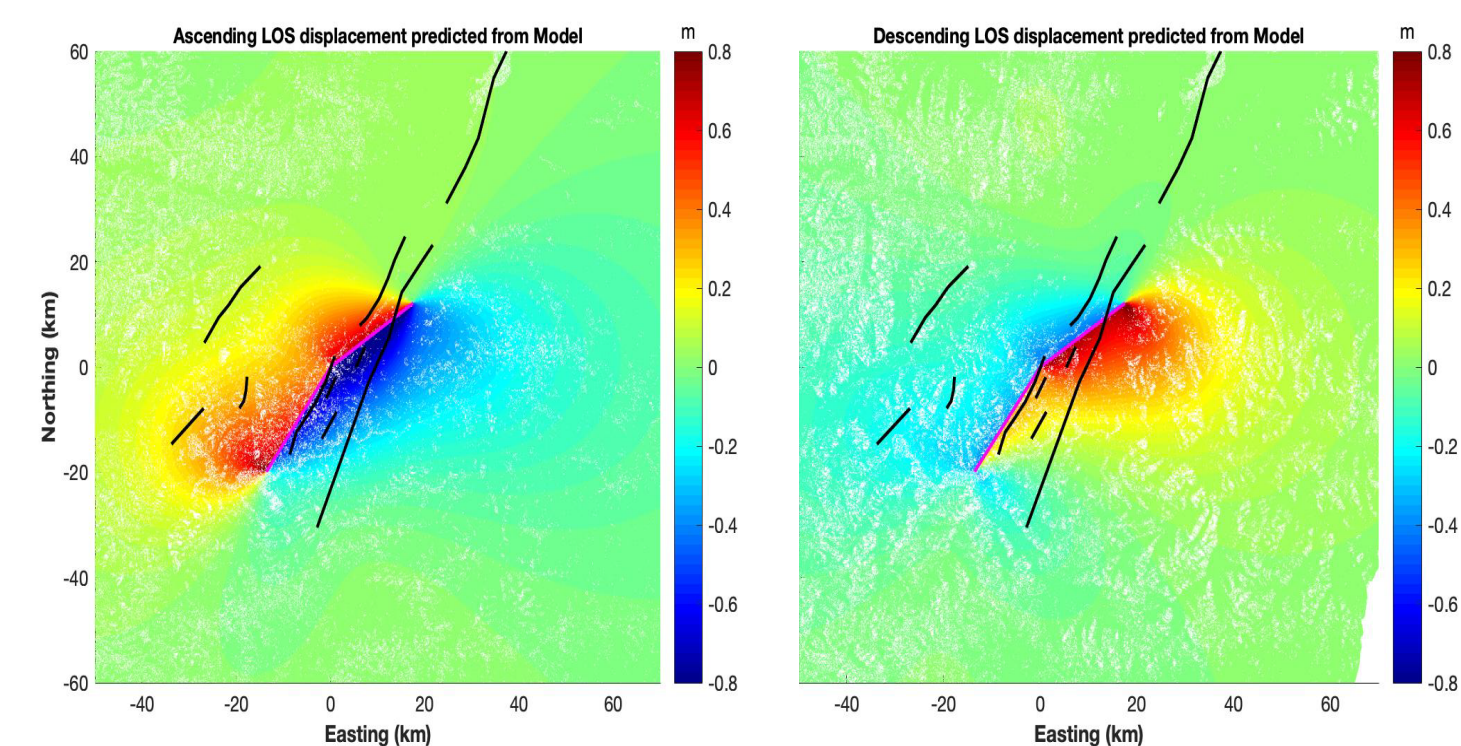## Models of Postseismic Relaxation
Poroelastic Rebound

Figure 5: We compute fully relaxed poroelastic deformation by differencing coseismic models using the drained (0.2) and undrained (0.25) Poisson's ratios. The predicted surface displacements are projected into their respective LOS. There is some similarity in the polarity of LOS displacements between the data and models, suggesting that poroelastic rebound may have contributed to the observed displacements.

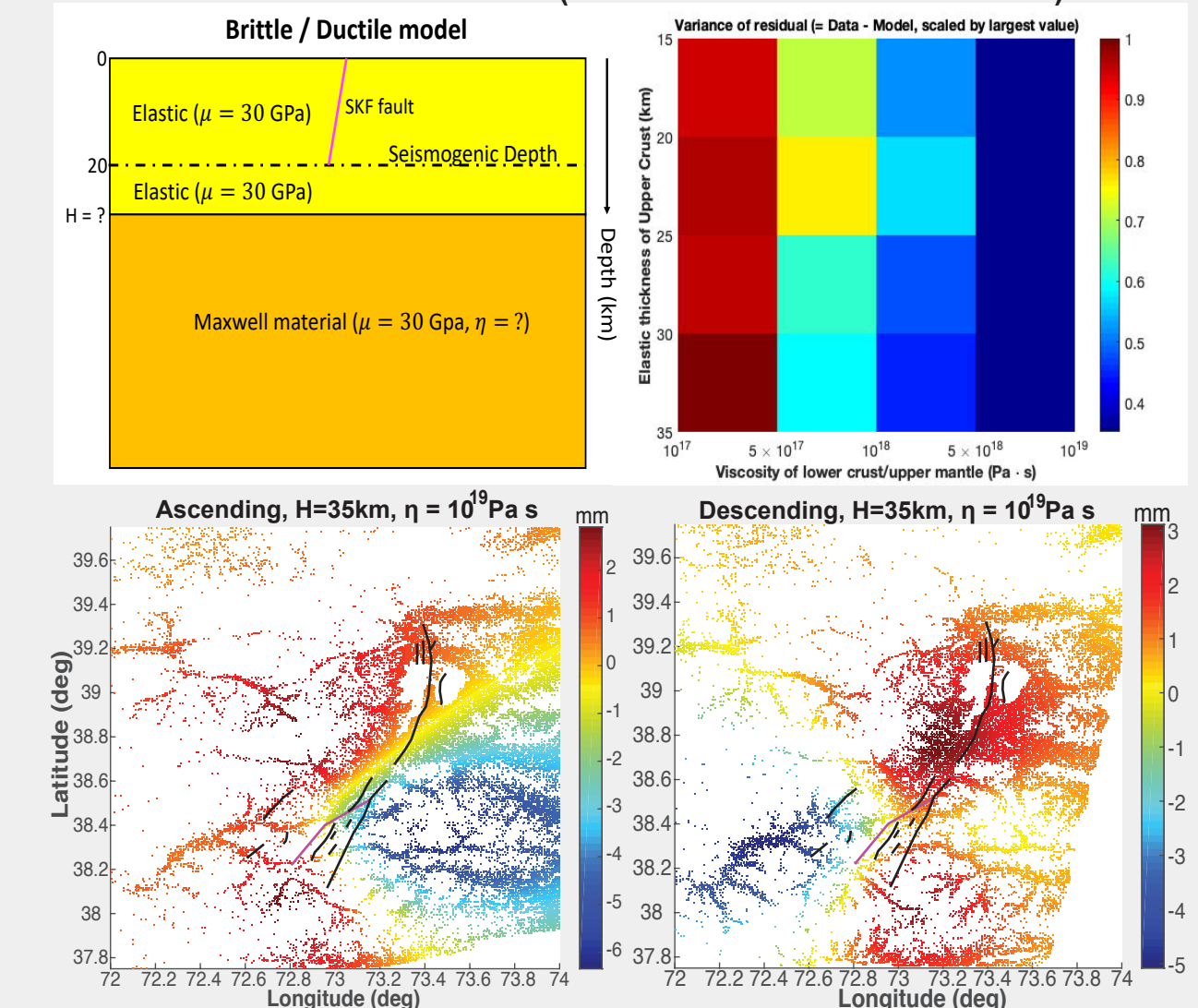### Visco-elastic Rebound (None of the models fits the data)

Figure 6: (Top left) A conceptual two-layer model of viscoelastic relaxation. We performed simulations over a range of assumed thicknesses of the elastic layer and viscosity of the underlying ductile substrate. Calculations were performed using PSGRN/PSCMP (Rongjiang et al.,2005). (Top right) Variance of the residual for a family of forward models with variable assumed viscosities of the substrate and thicknesses of elastic layer. (Bottom) Predictions of LOS displacements due to visco-elastic relaxation for H = 35km, η = 10^19 Pa s. Visco-elastic models predicted the long-wavelength signal, which is not seen in the data. Therefore, models that produce the smallest residuals are the ones with high viscosities (> 10^19 Pa s or larger). It follows that visco-elastic rebound does not significantly contributes to the observed deformation following the mainshock.